# Stability trends of MAX phases from first principles


Martin Dahlqvist, Björn Alling and Johanna Rosén





Original Publication:

Martin Dahlqvist, Björn Alling and Johanna Rosén, Stability trends of MAX phases from first principles, 2010, Physical Review B. Condensed Matter and Materials Physics, (81), 22, 220102.
http://dx.doi.org/10.1103/PhysRevB.81.220102

PHYSICAL REVIEW B **81**, 220102(R) (2010)

# Stability trends of *MAX* phases from first principles

M. Dahlqvist,* B. Alling, and J. Rosén
*Department of Physics, Chemistry, and Biology, IFM, Linköping University, SE-581 83 Linköping, Sweden*
(Received 18 March 2010; revised manuscript received 7 June 2010; published 23 June 2010)

We have developed a systematic method to investigate the phase stability of $M_{n+1}AX_n$ phases, here applied for $M$=Sc, Ti, V, Cr, or Mn, $A$=Al, and $X$=C or N. Through a linear optimization procedure including all known competing phases, we identify the set of most competitive phases for $n=1-3$ in each system. Our calculations completely reproduce experimental occurrences of stable *MAX* phases. We also identify and suggest an explanation for the trend in stability as the transition metal is changed across the 3*d* series for both carbon- and nitrogen-based systems. Based on our results, the method can be used to predict stability of potentially existing undiscovered phases.

DOI: 10.1103/PhysRevB.81.220102 PACS number(s): 64.75.−g, 81.05.Je, 71.15.Nc, 02.60.Pn

The *MAX* phases are a class of nanolaminated materials with the general composition $M_{n+1}AX_n$ ($n=1-3$), where $M$ is an early transition metal, $A$ is an $A$-group element, and $X$ is either carbon or nitrogen.[1,2] Lately, these compounds have attracted extensive attention due to their combination of both ceramic and metallic properties,[3] which makes them potentially useful in, e.g., high-temperature structural, electrical, and tribological applications. From a vast number of combinatorial possibilities of three *MAX* phase elements, approximately 60 phases have been synthesized to date. A majority are 211 phases ($n=1$) while $Ti_2AlC$ and $Ti_3SiC_2$ are the most well known and most studied.[4]

Theoretical studies related to *MAX* phase properties are numerous, ranging from investigations of, e.g., elastic properties to electronic-structure calculations.[5–11] Such work is relevant to gain knowledge and understanding of existing phases. However, surprisingly little has been done to reflect on whether or not studied phases not yet synthesized can be expected to exist experimentally. There are several relevant aspects of stability where one is the intrinsic stability, i.e., that the Gibbs free energy of the structure is in a local minimum with respect to small deformations. Recently Cover *et al.*[12] did a comprehensive study on 240 $M_2AX$ phases, where approximately 20 are intrinsically unstable. However, even if they are intrinsically stable, a phase does not necessarily exist since there are competing phases which might be thermodynamically favorable. Palmquist *et al.*[13] investigated the stability of $M_{n+1}AX_n$ phases in the Ti-Si-C system, by comparing the total energy of the *MAX* phases with the total energy of *ad hoc* chosen competing equilibrium phases. They found $n=1,2,3$ to be stable although $Ti_2SiC$ has not been observed experimentally.[13] Only recently, Keast *et al.*[14] did an ambitious study of the phase stability for a selection of $M_{n+1}AX_n$ phases ($n=1-4$), including $Ti_2SiC$, and found agreement with experiment.

In this work, we perform a systematic investigation of the phase stability of known as well as hypothetical *MAX* phases using first-principles calculations. An important subset of the $M_{n+1}AX_n$ elemental combinations is studied, where $M$=Sc, Ti, V, Cr, and Mn, $A$=Al, and $X$=C and N. In order to avoid *ad hoc* selected competing phases, careful investigations of phase diagrams and experimental work have been conducted in order to include all known, as well as some hypothetical, phases in each system, see, e.g., Refs. 15 and 16. In Table I, the phases included in this work are presented. Compounds with several phases are included in the form of their low-temperature thermodynamically stable phase, serving as a "lowest-energy" representation, and, as such, the most competitive phase. Furthermore, in order to make the correct, and in ternary and multinary systems nontrivial, choice of most competitive set of rivalrous phases, a linear optimization problem is solved.[17] As an example, we find the most competing phases for $Ti_2AlC$ to be $Ti_3AlC_2$ and TiAl in contrast to the *by-hand* identified combination $Ti_3AlC$, TiC, and $TiAl_3$ suggested by Keast *et al.*[14] Our systematic approach allows us to investigate trends in phase stability for compositionally different *MAX* phases.

All calculations are based on density-functional theory (DFT),[18] as implemented in the Vienna *ab initio* simulation package (VASP),[19,20] wherein the projector augmented wave[21] method and the generalized gradient approximation[22] for the exchange-correlation energy and one-electron potential are used. Reciprocal-space integration was performed within the Monkhorst-Pack scheme[23] with a plane-wave cut-off energy of 400 eV. The convergence was 0.1 meV for the total energy, and the $k$-point density was converged below 1 meV per formula unit, for each phase separately. All phases were optimized with respect to cell volume, $c/a$ ratio, as well as internal parameters. All Cr- and Mn-containing phases were allowed to be magnetic. Ferromagnetic as well as different antiferromagnetic structures were tested and the configuration with lowest total energy was included in the study.

The analysis of the phase stability has been divided in two parts, where the first concerns the formation enthalpy of $M_{n+1}AlX_n$ with respect to its non-*MAX* competing phases: single elements, binary, and other ternary compounds. In the second part, the $M_{n+1}AlX_n$ phases are compared to all known phases, including those with $M_{n+1}AlX_n$ structure. The latter to emphasize the possibility of $M_{n+1}AlX_n$ phases with different $n$ competing with each other.

Even if all known phases of a ternary phase diagram are taken into consideration, it is a nontrivial task to choose among them the most competitive set of rivalrous structures at each $M_{n+1}AlX_n$ composition.[17] Therefore, a systematic scheme to search for the most competitive combination of phases at a given elemental composition $b^M$, $b^A$, and $b^X$ was applied, using the simplex linear optimization procedure to solve the equation

 

TABLE I. Included phases in each *M-A-X* system. Phases in *italic* have not been found experimentally and are treated as hypothetical phases.

| *M* | *M-A* | *M-X* | *A-X* |
|---|---|---|---|
| Sc | $ScAl_3$, $ScAl_2$, B2-ScAl, $Sc_2Al$ | $Sc_3C_4$, ScC, $ScC_{0.875}$, $Sc_4C_3$, $Sc_2C$ | $Al_4C_3$ |
| | | ScN, $ScN_{0.875}$ | AlN |
| Ti | $TiAl_3$, $TiAl_2$, TiAl, $Ti_3Al$ | TiC, $TiC_{0.875}$, $Ti_2C$ | $Al_4C_3$ |
| | | TiN, $TiN_{0.875}$, $Ti_2N$ | AlN |
| V | $VAl_{10}$, $V_7Al_{45}$, $V_3Al_{10}$, $VAl_3$, $V_5Al_8$, $V_3Al$ | VC, $VC_{0.875}$, $V_6C_5$, $V_4C_3$, $\alpha$-$V_2C$, $\beta$-$V_2C$ | $Al_4C_3$ |
| | | VN, $VN_{0.875}$, $V_2N$ | AlN |
| Cr | $Cr_7Al_{43}$, $Cr_5Al_{21}$, $Cr_4Al_9$, $Cr_5Al_8$, $Cr_2Al$ | $Cr_3C_2$, $Cr_7C_3$, $Cr_3C$, $Cr_{23}C_6$ | $Al_4C_3$ |
| | | o-CrN, c-CrN, c-$CrN_{0.875}$, $Cr_2N$ | AlN |
| Mn | $MnAl_6$, $Mn_3Al_{10}$, $Mn_4Al_{11}$, MnAl, $Mn_7Al_{43}$ | MnC, $Mn_7C_3$, $Mn_5C_2$, $Mn_3C$, $Mn_{23}C_6$ | $Al_4C_3$ |
| | | MnN, $MnN_{0.875}$, $Mn_4N$, $Mn_3N_2$, $Mn_2N$ | AlN |

| *M* | *M-A-X* |
|---|---|
| Sc | *$Sc_2AlC$*, *$Sc_3AlC_2$*, *$Sc_4AlC_3$*, *$Sc_3AlC$*, $ScAl_3C_3$ |
| | *$Sc_2AlN$*, *$Sc_3AlN_2$*, *$Sc_4AlN_3$*, $Sc_3AlN$ |
| Ti | $Ti_2AlC$, $Ti_3AlC_2$, *$Ti_4AlC_3$*, c-$Ti_3AlC$, *o-$Ti_3AlC$* [a] |
| | $Ti_2AlN$, *$Ti_3AlN_2$*, $Ti_4AlN_3$, c-$Ti_3AlN$, o-$Ti_3AlN$ [a] |
| V | $V_2AlC$, $V_3AlC_2$, $V_4AlC_3$, $V_{12}Al_3C_8$, *$V_3AlC$* |
| | *$V_2AlN$*, *$V_3AlN_2$*, *$V_4AlN_3$*, *$V_3AlN$* |
| Cr | $Cr_2AlC$, *$Cr_3AlC_2$*, *$Cr_4AlC_3$*, *$Cr_3AlC$* |
| | *$Cr_2AlN$*, *$Cr_3AlN_2$*, *$Cr_4AlN_3$*, *$Cr_3AlN$* |
| Mn | *$Mn_2AlC$*, *$Mn_3AlC_2$*, *$Mn_4AlC_3$*, $Mn_3AlC$ |
| | *$Mn_2AlN$*, *$Mn_3AlN_2$*, *$Mn_4AlN_3$*, *$Mn_3AlN$* |

[a]$Re_3B$-type structure.

TABLE II. Calculated formation enthalpies $\Delta H_{comp}$ for $M_{n+1}AX_n$ phases including the most competing phases. $\Delta H_{comp}$ is calculated using Eq. (2). Phases with $\Delta H_{comp} < 0$ are in bold.

| | | $M_{n+1}AC_n$ | | $M_{n+1}AN_n$ | |
|---|---|---|---|---|---|
| *M* | *n* | Most competing phases | $\Delta H_{comp}$ (eV/atom) | Most competing phases | $\Delta H_{comp}$ (eV/atom) |
| Sc | 1 | $Sc_3AlC$, $ScAl_3C_3$ | 0.100 | ScN, $ScAl_2$, $Sc_3AlN$ | 0.088 |
| | 2 | $Sc_3AlC$, $Sc_3C_4$, $ScAl_3C_3$ | 0.155 | ScN, $ScAl_2$, $Sc_3AlN$ | 0.036 |
| | 3 | $Sc_3AlC$, $Sc_3C_4$, $ScAl_3C_3$ | 0.191 | ScN, $ScAl_2$, $Sc_3AlN$ | 0.020 |
| Ti | 1 | $Ti_3AlC_2$, TiAl | **−0.027** | $Ti_3AlN_2$, $TiAl_2$, o-$Ti_3AlN$ | **−0.050** |
| | 2 | $Ti_2AlC$, $Ti_4AlC_3$ | **−0.012** | $Ti_2AlN$, $Ti_4AlN_3$ | 0.013 |
| | 3 | $Ti_3AlC_2$, TiC | 0.000 | $Ti_3AlN_2$, TiN | **−0.022** |
| V | 1 | $V_2C$, $VAl_3$, $V_3AlC_2$ | **−0.072** | $V_2N$, $VAl_3$, AlN | 0.015 |
| | 2 | $V_2AlC$, $V_6C_5$, $Al_4C_3$ | **−0.005** | $V_2N$, AlN, $VAl_3$ | 0.154 |
| | 3 | $V_3AlC_2$, $V_6C_5$, $Al_4C_3$ | 0.006[a] | $V_2N$, AlN | 0.204 |
| Cr | 1 | $Cr_2Al$, $Cr_3C_2$, $Al_4C_3$ | **−0.067** | Cr, AlN | 0.353 |
| | 2 | $Cr_2AlC$, $Cr_3C_2$, C | 0.079 | Cr, $Cr_2N$, AlN | 0.324 |
| | 3 | $Cr_2AlC$, $Cr_3C_2$, C | 0.106 | $Cr_2N$, AlN | 0.306 |
| Mn | 1 | MnAl, C, $Mn_3AlC$ | 0.005 | Mn, AlN | 0.376 |
| | 2 | C, $Mn_3AlC$ | 0.094 | $Mn_2N$, $Mn_4N$, AlN | 0.363 |
| | 3 | C, $Mn_3AlC$, $Mn_{23}C_6$ | 0.153 | $Mn_2N$, AlN | 0.311 |

[a]$\Delta H_{comp} = -0.012$ eV/atom with 11% vacancies on the carbon sublattice in a $V_{12}Al_3C_8$ structure (Ref. 27).

$$\min E_{comp}(b^M,b^A,b^X) = \sum_i^n x_i E_i, \quad (1)$$

where $x_i$ and $E_i$ is the amount and energy of compound $i$, respectively. $E_{comp}$ is the energy that should be minimized subject to the constraints

$$x_i \geq 0; \quad \sum_i^n x_i^M = b^M, \sum_i^n x_i^A = b^A, \sum_i^n x_i^X = b^X,$$

where $x_i^M$ is the amount of $M$ atoms in $x_i$ of compound $i$, etc. For the $M_{n+1}AX_n$ composition, $b^M=n+1$, $b^A=1$, and $b^X=n$. The formation enthalpy with respect to the identified most competitive combination of phases is thus calculated according to

$$\Delta H_{comp}(M_{n+1}AX_n) = E(M_{n+1}AX_n) - E_{comp}(b^M,b^A,b^X), \quad (2)$$

where the term $E_{comp}$ is given by Eq. (1).

$M_{n+1}AlX_n$ phase formation enthalpies based on all non-*MAX* competing phases are summarized in Fig. 1. Panel (a) shows the formation enthalpies, $\Delta H_{elements}$, with respect to only the pure elements in their most stable structure. In this comparison, the nitrogen containing $M_{n+1}AlX_n$ phases would have a maximum stability with Sc as $M$ element. In the carbon case, $\Delta H_{elements}$ displays a clear minimum with Ti as $M$ element. However, these trends change, see panel (b), when applying the relevant stability criteria $\Delta H_{comp}$, including comparison also to binaries and other ternary phases (excluding competing *MAX* phases). The nitrogen *MAX* phases now display a minimum in the region of Ti as $M$ element while the carbon *MAX* phases has a minimum around $M$ =V for $n=1$ and in between Ti and V for $n=2$ and 3. As $n$ increases the identified minima for $\Delta H_{comp}$ is shifted slightly to the left which is influenced by the addition of the energetically favorable $MX$ block (most pronounced for $M$=Ti) in the $M_{n+1}AX_n$ phase. No Sc or Mn-based *MAX* phase has a negative $\Delta H_{comp}$. To explain the shift in trends between panels (a) and (b) in Fig. 1 we need to look at the stabilities of the competing phases, especially the binaries with $M$C, $M$N, and $M$Al stoichiometry (or corresponding combinations, e.g., $V_6C_5$+C=VC). These are shown in panel (c). The $M$N binaries shows a minimum value of $\Delta H_{elements}$ at $M$=Sc, which corresponds to filling the bonding electronic states in the rocksalt structure. Approximately the same band filling is obtained at $M$=Ti in the carbide TiC, also rocksalt.[24] $\Delta H_{elements}$ of the metal-aluminum compounds show smaller variations as the transition metal is changed. The similarities in the trends of $\Delta H_{elements}$ of *MAX* phases, panel (a), and the $M$N and $M$C binaries, panel (c), suggest that the bonding physics of the $MX$ layers of the *MAX* phases are similar to the case in, e.g., rocksalt transition-metal nitrides and carbides in line with soft x-ray spectroscopy experiments.[25,26] Thus, the competition with $MX$ binaries in panel (c) shifts the stability maxima of the *MAX* phases to higher valence in $M$, as seen by comparing $\Delta H_{elements}$ in panel (a) and $\Delta H_{comp}$ in panel (b). Furthermore, for the nitrogen-based $M_{n+1}AX_n$ phases, AlN enters as a highly competing phase for the higher valence systems ($M$=V, Cr, and Mn) giving rise to a substantial difference between $\Delta H_{comp}$ of the carbide and nitride *MAX* phases in these cases. The high stability of AlN (in comparison to the lower stability of $Al_4C_3$) may explain why so few nitride $M_{n+1}AlN_n$ phases have been synthesized.

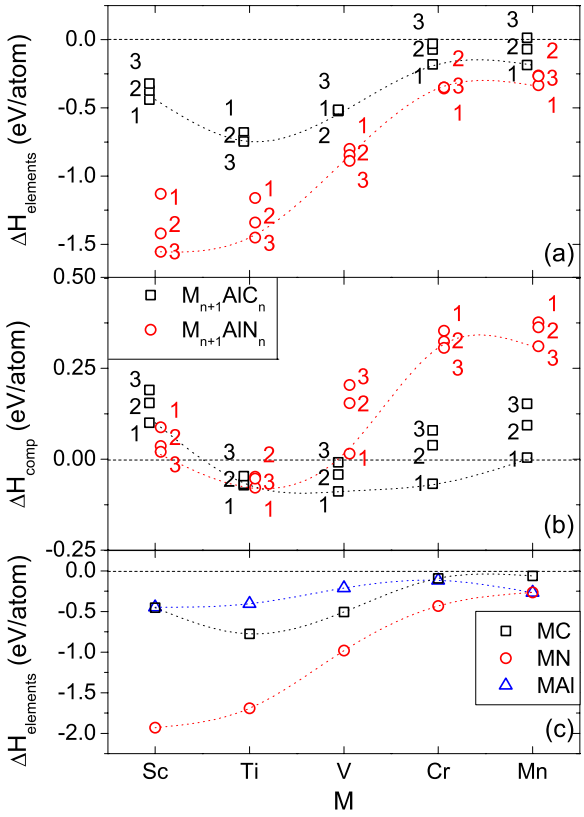


FIG. 1. (Color online) Calculated formation enthalpy of $M_{n+1}AlX_n$ with respect to (a) its single elements and (b) most competing phases using Eqs. (1) and (2) (competing *MAX* phases not included). $X$ is either C (black square) or N (red circle), and $A$ is Al. Phases with $n=1$ ($M_2AX$) are marked as 1, $n=2$ ($M_3AX_2$) as 2, and $n=3$ ($M_4AX_3$) as 3. (c) Calculated formation enthalpy of binaries (or combinations corresponding to binaries) of $M$C, $M$N, and $M$Al stoichiometries with respect to its single elements. Dotted lines serve as guide for the eye.

These results illustrate the importance of including all competing phases, not only single elements, to elucidate trends in phase stabilities. In addition to the result in panel (b) of Fig. 1, a full comparison including also competing *MAX* phases have been performed. In Table II, resulting $\Delta H_{comp}$ as well as the most competitive combination of phases for $M_{n+1}AX_n$ is presented. Note that only seven $M_{n+1}AX_n$ phases have $\Delta H_{comp}<0$, in comparison to the ten phases in panel (b) of Fig. 1. Comparing these results to experimentally known phases, see Table III, the only discrepancy was initially found for $V_4AlC_3$ with $\Delta H_{comp}$ =0.006 eV/atom. This inconsistency might be correlated to observed C site vacancies of approximately 11%.[27] A corresponding superstructure of $V_{12}Al_3C_8$ was therefore taken into consideration, resulting in phase stabilization of $\Delta H_{comp}$=−0.012 eV/atom, as compared with the most competing set of phases $V_2AlC$ and $V_6C_5$.

As a complement to Table II, the competition between different $M_{n+1}AX_n$ phases is illustrated by calculating $\Delta H_{comp}$ relative to $MX$ and $MA$ stoichiometry along a line across the

TABLE III. *MAX* phases with calculated negative formation enthalpy ($\Delta H_{comp}<0$), compared to experimentally observed *MAX* phases within the herein investigated systems.

| *MAX* with $\Delta H_{comp}<0$ | Experimentally observed *MAX* phases[a] |
|---|---|
| $Ti_2AlC$, $Ti_3AlC_2$, *$Ti_4AlC_3$* [b] | $Ti_2AlC$, $Ti_3AlC_2$ |
| $V_2AlC$, $V_3AlC_2$, $V_4AlC_3$ [c] | $V_2AlC$, $V_3AlC_2$, $V_4AlC_3$ |
| $Cr_2AlC$ | $Cr_2AlC$ |
| $Ti_2AlN$, $Ti_4AlN_3$ | $Ti_2AlN$, $Ti_4AlN_3$ |

[a]Reference 4.
[b]$Ti_4AlC_3$ have $\Delta H_{comp}=0.000$ eV/atom to the level of accuracy in our work.
[c]11% carbon vacancies stabilize the 413 *MAX* phase as observed in Ref. 27.

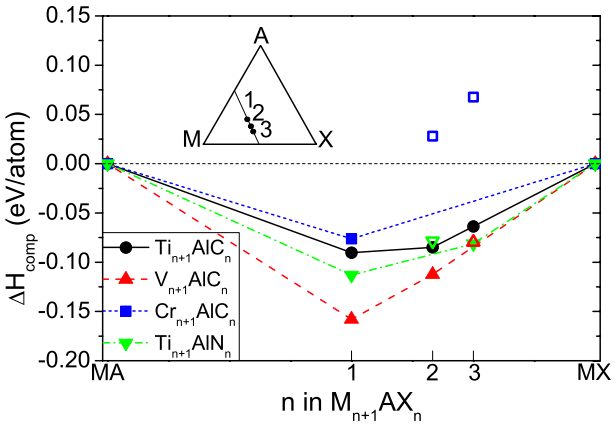


FIG. 2. (Color online) Formation enthalpy of $M_{n+1}AX_n$ with respect to binaries of *MX* and *MA* stoichiometry. Filled symbols represent stable phase and hollow symbols those considered unstable. The inset shows the position of the $M_{n+1}AX_n$ phases on the line between *MX* and *MA* in the phase diagram.

phase diagram, see Fig. 2. Included are the four ternary systems shown in panel (b) of Fig. 1, where at least one $M_{n+1}AX_n$ phase has $\Delta H_{comp}<0$. Note that phases with filled symbols in Fig. 2 are considered stable whereas those with hollow symbols are considered unstable. An explanation to why $Ti_3AlN_2$ has not been found experimentally is given through its higher formation enthalpy as compared with a combination of $Ti_2AlN$ and $Ti_4AlN_3$. Looking at $Ti_4AlC_3$, it is found on the line between $Ti_3AlC_2$ and TiC and can be considered as a borderline case, possibly unstabilized by $TiC_x$ off-stoichiometry. It is also found that $V_4AlC_3$ is unstable relative to $V_3AlC_2$ and VC (corresponding to $V_6C_5$ +C), though as mentioned earlier carbon vacancies can stabilize a 413-*like MAX* phase. When comparing the here identified stable $M_{n+1}AX_n$ phases, i.e., those with $\Delta H_{comp}<0$ in Table II and Fig. 2, with experimentally known $M_{n+1}AX_n$ phases as presented in Table III, the complete reproduction of experimental occurrence demonstrate the strength and potential of our approach.

In conclusion, we have investigated the phase stability of $M_{n+1}AX_n$ phases using DFT calculations in combination with linear optimization procedures. We identify and suggest an explanation to the here observed trend in phase stability as the transition metal is changed across the 3*d* series. For carbon containing *MAX* phases, a maximum stability is reached around V as transition metal, while for nitrogen, a maximum stability is reached for Ti. Even though the calculations are for 0 K, the calculated phase stability reflects experimental occurrence very well, which indicates that the formation of $M_{n+1}AX_n$ are mainly governed by the total energy term in the Gibbs free energy, although for borderline cases the vibrational effects comes into play at high temperatures.[28] $M_{n+1}AX_n$ phases are highly ordered compounds where a considerable energetic driving force and sufficient diffusion is needed to stabilize the structure during synthesis. This explains the remarkable agreement between our predictions and the experimentally reported phases, and indicates a considerable challenge in synthesizing metastable $M_{n+1}AX_n$ phases. Furthermore, our method is a reliable tool that can be used as guidance for further search of new $M_{n+1}AX_n$ phases, as well as other multinary compounds, before time consuming and expensive experimental investigations are attempted.

Financial support from the Swedish Foundation for Strategic Research (SSF), and the Swedish Research Council (VR) is gratefully acknowledged. All simulations were carried out using allocations provided by the Swedish National Infrastructure for Computing (SNIC).

*madah@ifm.liu.se

[1] V. H. Nowotny, Prog. Solid State Chem. **5**, 27 (1971).
[2] M. W. Barsoum, Prog. Solid State Chem. **28**, 201 (2000).
[3] M. W. Barsoum and T. El-Raghy, Am. Sci. **89**, 334 (2001).
[4] P. Eklund *et al.*, Thin Solid Films **518**, 1851 (2010).
[5] Y. Zhou and Z. Sun, Phys. Rev. B **61**, 12570 (2000).
[6] G. Hug and E. Fries, Phys. Rev. B **65**, 113104 (2002).
[7] S. E. Lofland *et al.*, Appl. Phys. Lett. **84**, 508 (2004).
[8] Z. Sun *et al.*, Solid State Commun. **129**, 589 (2004).
[9] J. Wang and Y. Zhou, Phys. Rev. B **69**, 214111 (2004).
[10] M. F. Cover, *et al.*, Adv. Eng. Mater. **10**, 935 (2008).
[11] J. M. Wang *et al.*, Acta Mater. **56**, 1511 (2008).
[12] M. F. Cover *et al.*, J. Phys. Condens. Matter **21**, 305403 (2009).
[13] J. P. Palmquist *et al.*, Phys. Rev. B **70**, 165401 (2004).
[14] V. J. Keast *et al.*, Phys. Rev. B **80**, 214113 (2009).
[15] T. B. Massalski, in *Binary Alloy Phase Diagrams* (ASM International, Metals Park, Ohio, 1986), Vol. 1 and 2.
[16] J. C. Schuster and J. Bauer, J. Solid State Chem. **53**, 260 (1984).
[17] M. Dahlqvist *et al.*, Phys. Rev. B **81**, 024111 (2010).
[18] P. Hohenberg and W. Kohn, Phys. Rev. **136**, B864 (1964).
[19] G. Kresse and J. Hafner, Phys. Rev. B **48**, 13115 (1993).
[20] G. Kresse and J. Hafner, Phys. Rev. B **49**, 14251 (1994).
[21] P. E. Blöchl, Phys. Rev. B **50**, 17953 (1994).
[22] J. P. Perdew *et al.*, Phys. Rev. Lett. **77**, 3865 (1996).
[23] H. J. Monkhorst and J. D. Pack, Phys. Rev. B **13**, 5188 (1976).
[24] J. Häglund *et al.*, Phys. Rev. B **48**, 11685 (1993).
[25] M. Magnuson *et al.*, Phys. Rev. B **76**, 195127 (2007).
[26] M. Magnuson *et al.*, Phys. Rev. B **74**, 195108 (2006).
[27] J. Etzkorn *et al.*, Inorg. Chem. **46**, 7646 (2007).
[28] D. Music *et al.*, J. Phys.: Condens. Matter **19**, 136207 (2007).